Turk J Phys
30 (2006) , 335 – 344.
© TÜBİTAK

A Detailed Ensemble Monte Carlo Study of the Effect of Quantum Well Width on Quantum Well Infrared Photodetector Characteristics

S. MEMİŞ[1], O. O. CELLEK[2], U. BOSTANCI[1], M. TOMAK[1], C. BEŞİKÇİ[2]
[1]*Department of Physics, Middle East Technical University,*
06531, Ankara, TURKEY
e-mail: smemis@photon.physics.metu.edu.tr
[2]*Department of Electrical Engineering, Middle East Technical University,*
06531 Ankara-TURKEY

Received 18.07.2006

Abstract

We present a simulation based investigation of the dependence of the device characteristics on the quantum well width in AlGaAs/GaAs quantum well infrared photodetectors (QWIPs) through the ensemble Monte Carlo technique. The simulations on two different standard $Al_{0.3}Ga_{0.7}As$/GaAs QWIPs with quantum well widths of 36 and 44 Å have shown that the gain in the former is considerably higher, which is due to much longer lifetime of the photoexcited electrons as a result of lower capture probability in the device. We discuss this observation by the investigation of the electron scattering rates in these structures through realistically evaluated scattering mechanisms between two and three-dimensional states in the multi-quantum well structure.

Key Words: Quantum well infrared photodetectors

1. Introduction

As a challenging alternative to the conventional intrinsic infrared photodetectors, quantum well infrared photodetector (QWIP) technology has matured rapidly, and very large format QWIP focal plane arrays have already been reported [1, 2]. Advantages such as low production cost, tunable spectral band, radiation-hardness and the possibility of monolithic integration with the peripheral electronics make the QWIP attractive for infrared sensing applications.

There has been a considerable amount of experimental and theoretical work toward a better understanding of QWIP operation and the underlying physics. Although this unipolar photoconductor has a simple layer structure, precise QWIP modeling is a difficult task. The transport of the continuum electrons under far from equilibrium conditions needs sophisticated models that should also account for the reflection of electrons at the quantum well (QW) locations. Furthermore, an accurate description of the capture and emission mechanisms requires realistically modeled scattering rates between two dimensional (2D) and three dimensional (3D) states.

There have been many studies on analytical modeling of QWIPs, as well as numerical modeling based on the drift-diffusion model of electron transport [3–13]. However, the well-known limitations of the drift-diffusion model may result in incorrect prediction of the device characteristics [14]. The hydrodynamic transport models are more reliable than the drift-diffusion formulation for the simulation of semiconductor devices, but the application of this method to QWIPs is not simple. In this approach, the energy dependent

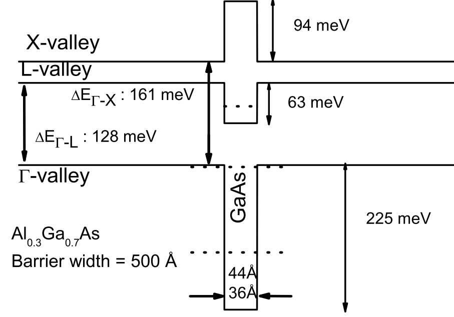

Figure 1. Details of the energy band diagram for $Al_{0.3}Ga_{0.7}As/GaAs$.

parameters are obtained from Monte Carlo simulations on bulk material. For a multi quantum well (MQW) structure, extraction of these parameters is much more complicated, since vertical transport through a MQW structure is considerably different than that in bulk material.

Ensemble Monte Carlo (EMC) method [15] is an efficient way for investigating QWIP operation and characteristics. The EMC method is also a useful tool for optimizing the QWIP structure for better performance. There have been several reports on the QWIP MC simulations [14, 16, 17, 18, 19, 20, 21, 22, 23, 24]. The previous works enlightened various important features of QWIP operation. However, there are still questions to be answered for better understanding of QWIP operation and characteristics.

In this paper, we report the results of our work on the detailed EMC simulation of standard QWIPs. We concentrate our work on the dependence of the device characteristics on the quantum well width for standard QWIP structures with typically long quantum wells. With this main objective, we simulated two different standard $Al_{0.3}Ga_{0.7}As/GaAs$ QWIPs with quantum well widths of 36 and 44 Å. The results suggest that the photoexcited electron lifetime in the device with 36 Å thick quantum well is considerably higher than that in the other as a result of lower capture probability (p_c), in the device.

Section 2 summarizes the simulation procedure. Section 3 includes presentation and discussion of the results, and the conclusion is given in section 4.

2. Simulation Details

We simulated $Al_{0.3}Ga_{0.7}As/GaAs$ QWIPs in the standard structure with two different quantum well lengths of 36 and 44 Å. The simulated structure has 16 GaAs quantum wells sandwiched between 500 Å thick $Al_{0.3}Ga_{0.7}As$ barriers. The QW n-type doping density is selected to be 1.76×10^{11} cm^{-2} in both QWIPs [25]. Material and heterostructure parameters are taken from several sources [26, 27, 28], and band nonparabolicities are taken into account. The details of the energy band diagram are given in Figure 1.

In our EMC simulations, both three-dimensional (3D) and two-dimensional (2D) electrons are simulated by taking size quantization into account in Γ- and L-valleys of the conduction band. The rates of the presumably important 2D↔2D and 2D↔3D scattering processes are evaluated using the solutions of the Schrödinger's Equation.

The mechanisms included in the simulation are polar optical phonon (POP), acoustic phonon, ionized impurity, alloy, and intervalley (equivalent and nonequivalent) scatterings. Electron-electron scattering which will presumably be important at higher QW electron concentrations is ignored.

$Al_xGa_{1-x}As$ with $x \sim 0.3$ is mostly used as the barrier material in long wavelength infrared (LWIR) QWIPs. A significant portion of the barrier electrons in such devices resides in the L valley of the conduction band under typical bias voltages due to the small energy spacing between the central and satellite valleys in $Al_xGa_{1-x}As$ with the above composition. Moreover, POP emission rate in this valley is higher than that in Γ, and the continuum electrons in Γ valley have higher kinetic energy due to faster heating during their

transport in the barriers. As a result, electron capture through L-valley QW (L-QW) may significantly affect the characteristics of the QWIPs with the above barrier composition. Indeed, we revealed the dominance of electron capture through the L-valley by tracking the electrons which reach the GaAs well regions [29, 30]. It was observed that the percentage of the electrons entering the GaAs well regions in L valley that are eventually captured into Γ-valley QW may be an order of magnitude larger than that of the electrons entering the well regions in Γ-valley under typical bias voltages in the $Al_{0.3}Ga_{0.7}As$ /GaAs QWIP structure [29]. Therefore, reasonably precise evaluation of the scattering rates between the states in the central and satellite valleys of the conduction band is necessary for accurate simulation of the capture mechanism in QWIPs.

In the simulation program utilized in this work [29], the transitions of the electrons between the continuum and bound states ($\Gamma_{3D} \leftrightarrow \Gamma_{2D}$ and $L_{3D} \leftrightarrow L_{2D}$) are modeled as 3D↔2D POP scattering following the approach of Khalil et al. [31]. The 2D↔2D, and 3D↔2D scattering rates are calculated using the solutions of the Schrödinger's Equation. The wavefunctions and scattering rates are calculated once at the beginning of the simulation because of extreme time consumption during the calculation of the scattering rates throughout the simulation [32].

The 2D↔2D and 3D↔2D intervalley scattering rates between Γ and the higher energy valleys are calculated by using the approaches of Educato *et al.* [33] and Goodnick and Lugli [34]. Dielectric screening effects are included in the calculation of 2D POP scattering rates [35]. Electron tunneling through the emitter contact and the X-valley barrier in GaAs layers, and the quantum mechanical reflection/transmission of electrons by the heterointerfaces are also considered in the simulation [36, 37].

The simulated structure is divided into 4 Å long mesh cells. Poisson equation is solved within 20 fs time intervals using a finite difference scheme. Cloud in the Cell (CIC) method [38] is employed for mesh charge assignment. The details of the simulator can be found in [29].

The simulations were performed at the device temperature of 77 K and under the photoexcitation rate of 10^{10} s^{-1}. Simulation of QWIP with the EMC technique under low photoexcitation rates is impractical since large amount of computer time is needed to reach steady-state. Under the selected photoexcitation rate, the simulation reaches steady state in several nanoseconds beyond which, no significant change occurs in the observed quantities. Under this selected photoexcitation rate, barrier electron density is low enough so that the electric field distribution is not significantly affected by the high photoexcitation. The selected photoexcitation rate is also small enough to avoid saturation of inter-subband absorption [39]. Furthermore, this work focuses on the transport and capture of the excited carriers. Thermally excited and photoexcited carriers are expected to have similar energy distributions and properties [40].

3. Results and Discussion

3.1. Gain Characteristics

The QWIP gain can be expressed as L_d/L where L_d denotes the drift distance of the excited electrons, and L is total device length. Figure 2 shows the calculated drift distance and the experimentally obtained drift distance [40] on an $Al_{0.26}Ga_{0.74}As$/GaAs QWIP vs. average electric field in device. There is negative differential change (NDC) in the gain. The NDC was attributed to ground state tunneling by Levine et al. [41], whereas it was explained by intervalley transfer of the electrons in the barriers by Schneider et al. [40]. The ground state tunneling is not considered in our simulator.

Gain starts to increase with bias under large biases (above ∼3 V). Experimental results which are obtained through noise measurements have shown similar behavior [42, 43, 44]. This was previously attributed to avalanche multiplication [42, 43, 44], which is not included in our simulator. Our results suggest that the experimentally observed increase in the gain with increasing bias can partially be attributed to avalanche multiplication.

The quantum well length is an important variable which affects the characteristics of QWIPs. The drift distance increases as the well length is shortened from 44 to 36 Å. While there is a slight change in the average electron velocity in QWIPs with shorter well width, longer lifetime of the excited electrons, as seen in Figure 3, causes longer drift distance for the structure with shorter well length. The longer lifetime can be explained by the large decrease in local capture probability.

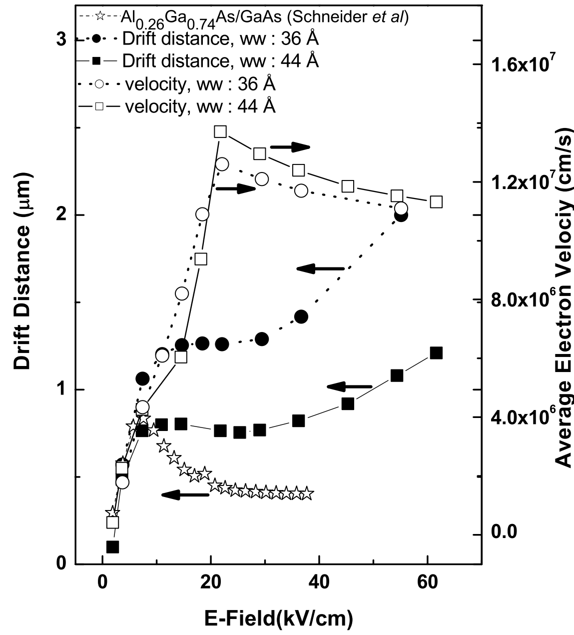

Figure 2. Calculated average electron velocity, drift distance and drift distance extracted from measured gains [40] versus average electric field in device

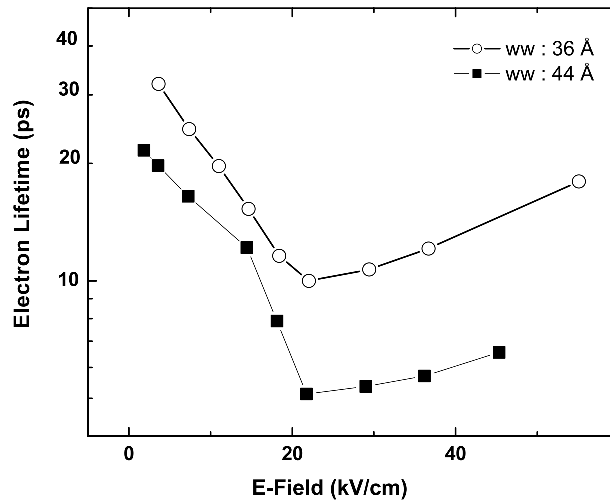

Figure 3. Average electron lifetime versus electric field in $Al_{0.3}Ga_{0.7}As/GaAs$ QWIPs with 36 and 44 Å well widths.

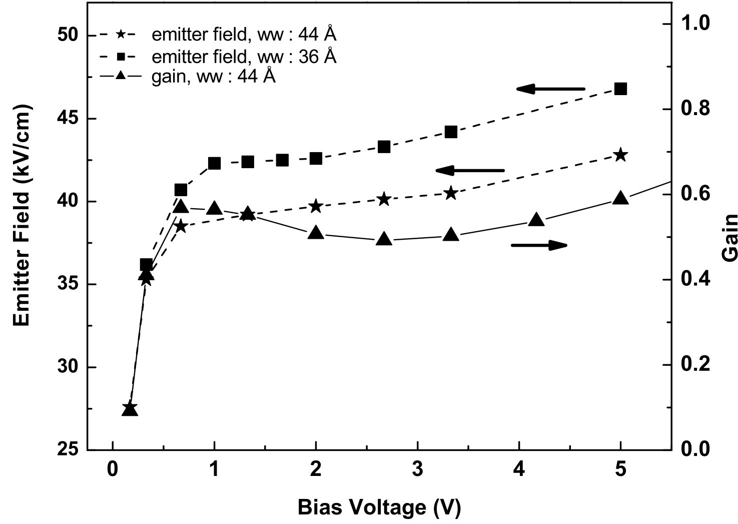

Figure 4. Calculated bias dependence of the emitter field and gain.

3.2. Electric Field and Electron Velocity Distribution

Electrons are injected into QWIP through tunneling at the emitter contact. The total current in bulk of the device determines the emitter field; so the increase in the emitter field with bias depends on the drift distance. The variation of the emitter field and gain with bias are illustrated in Figure 4.

NDC is not observed in the emitter field characteristics. Rather, the rate of increase in the emitter field decreases under moderate bias where there is strong NDC in the gain. Electric field distributions in the simulated devices are given in Figure 5. The rate of increase at the emitter field with bias decreases by the effect of the NDC in the gain. Although, the average velocity decreases slightly under high bias as seen in Figure 2, gain and the emitter field increase with almost equal rate which is due to the increase in the lifetime of electrons.

The current injected from the emitter field, together with local p_c, influence the charge densities in wells and barriers. The difference between the electric fields in the barriers neighboring the wells is determined by the charge in each well. Under large photoexcitation rate and small bias, there is large charge density in the barriers with low drift velocity. Under small bias, most of the bias voltage drops on a small region near the emitter, and the electric field in the rest of device is weak, as previously suggested [8, 45]. The rate of increase of the emitter field with bias is not the same as that in the bulk due to the different transport mechanisms.

As shown in Figure 5, accumulation starts to appear in the wells near the emitter as the applied bias increases enough to create large electric fields in the bulk. The non-uniform accumulation indicates non-uniform p_c. The well accumulation occurs in the wells near the emitter. Figure 6 shows the energy band diagrams and of the simulated 16-well $Al_{0.3}Ga_{0.7}As/GaAs$ QWIPs under various bias voltages. More uniform electric field is created throughout the device in the QWIP with shorter well width due to more uniform local p_c.

The change in the average barrier electron velocity with bias throughout the device is given in Figure 7 for 44 Å well width. In the barriers near the emitter, the average barrier velocity does not change significantly (under 0.33-3.33 V) since the electric field itself does not change considerably (~35-45 kV/cm). The higher value of average velocity on the first barrier means that most of the electrons lie in Γ-valley with high energy. In the bulk region, under 0.33V, the uniform and small electron velocity is a result of a uniform and small

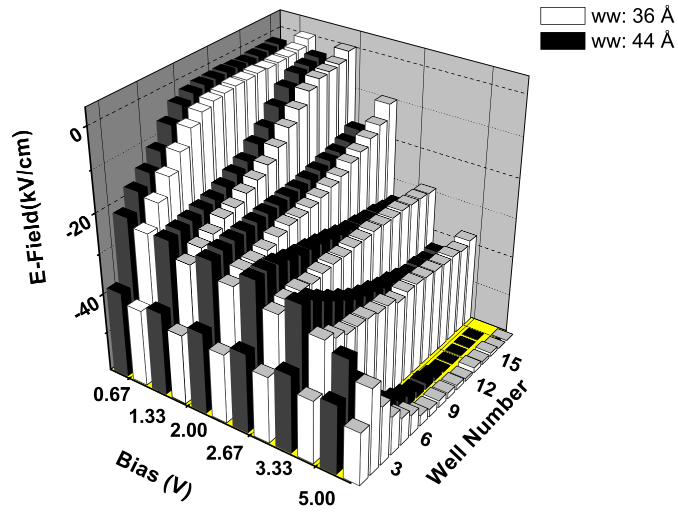

Figure 5. Calculated bias dependence of the emitter field and gain.

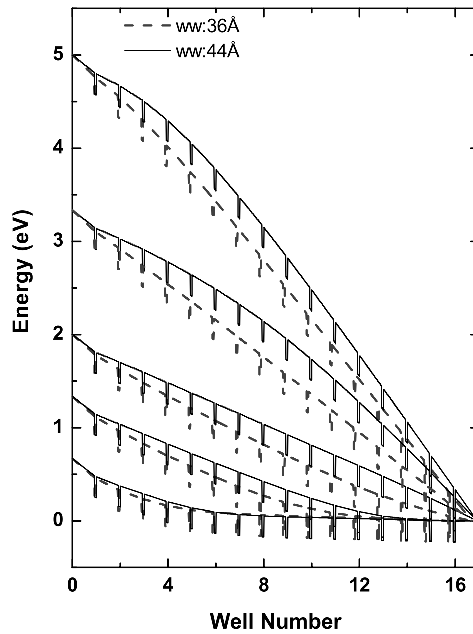

Figure 6. Energy band diagram in $Al_{0.3}Ga_{0.7}As$/GaAs QWIPs with 36 and 44 Å well widths.

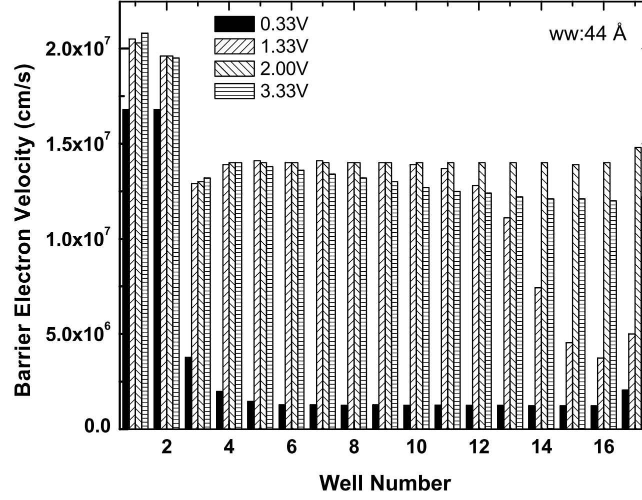

Figure 7. Average electron velocity in barriers in the QWIP structure with 44 Å well width.

electric field (~5 kV/cm), as seen in Figure 5. The average velocity saturates beyond the third barrier under sufficiently large bias. The electric field is distributed nearly uniformly under 2V bias, and the average velocity is uniform throughout the bulk region with the saturated value.

3.3. Scattering Rates and Local Capture Probability

The effects of shortening the quantum well width are different on different scattering rates. The capture and escape rates are shown in Figure 8. We can conclude that the scattering rates change in a way that capture events decrease with shortening well width from 44 to 36 Å.

When capturing via L-valley is not taken into account, it is supposed that the p_c decreases with electric field. Electrons in the Γ-valley have large kinetic energy due to faster heating in the barrier and their high momentum in growth direction decreases the p_c. In $Al_xGa_{1-x}As/GaAs$ with ~0.3 mole fraction, the energy separation between Γ- and L-valleys are close which increases the electron population in L-valley. The L-QW might affect the transport significantly since captured electrons cool in this well, then they can be scattered to the Γ-QW.

Local p_c, which is calculated by dividing the portion of the current captured by a well to the total current incident on the well, is illustrated in Figure 9. An increase in p_c with increasing electric field is observed under intermediate E- fields (~10-20 kV/cm)in 44 Å well width device where electron density in L-valley increases abruptly and the L-valley occupancy reaches ~ 40%. This increase is less significant in the shorter well width device. The p_c decreases under higher E- fields where the electrons in the satellite valleys reach high energy levels. The local p_c is almost halved for the structure with shorter well width.

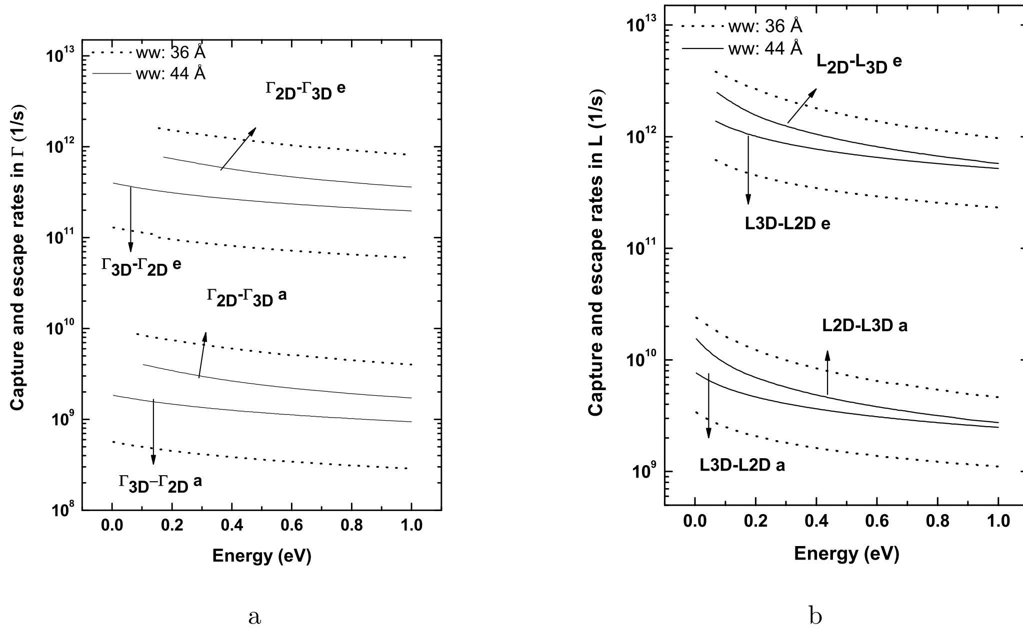

Figure 8. Capture and escape scattering rates a.) in -valley b.) in L-valley.

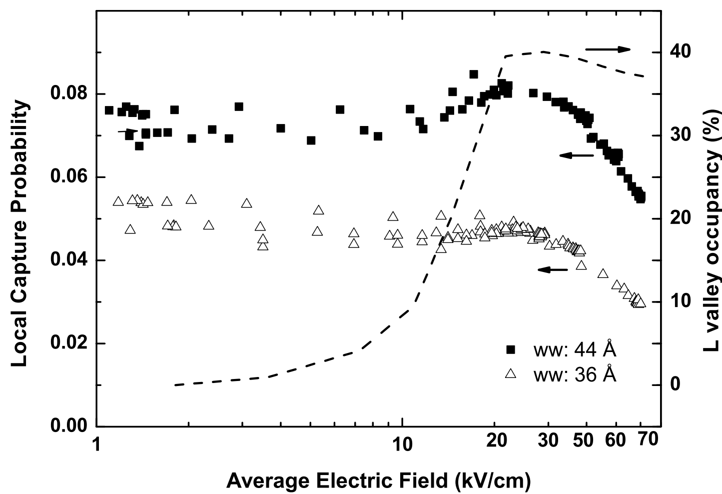

Figure 9. Calculated local capture probability for $Al_{0.3}Ga_{0.7}As/GaAs$ QWIPs with 36 and 44 Å well widths and L-valley occupancy for the same structure with 44 Å well width.

4. Conclusion

We present an investigation of the QWIP through EMC simulations. A quantitative explanation of the different gain-bias characteristics is given in QWIPs based on two different well widths, 36 and 44 Å. Simulation results show that shortening the well width of $Al_{0.3}Ga_{0.7}As/GaAs$ structure from 36 and 44 Å. increases the gain. The local p_c is almost halved under moderate bias when the well width is decreased.

Acknowledgments

This work is supported by Middle East Technical University Research Fund through Project No: BAP-2002-01-05-07 and the Scientific and Technical Research Council of Turkey (TUBITAK) under Contact No. 101E001.

References

[1] B. F. Levine, *J. Appl. Phys.*, **74**, (1993), R1.

[2] H. C. Liu, *Semiconductors and Semimetals*, ed. H. C. Liu and F. Capasso, vol. 62 (Academic Press, San Diago, 2000) p. 129.

[3] K. K. Choi, *The Physics of Quantum Well Infrared Photodetectors*, (Singapore: World Scientific, 1997), p.279.

[4] H. C. Liu, *Appl. Phys. Lett.*, **60**, (1992), 1507.

[5] V. Ryzhii, *J. Appl. Phys. Lett.*, **81**, (1997), 6442.

[6] M. Ershov, S. Satou and Y. Ikebe, *J. Appl. Phys. Lett.*, **86**, (1999), 6442.

[7] M. Ryzhii, I. Khmyrova, and V. Ryzhii, *IEEE Trans. Electron. Devices*, **45**, (1998), 293.

[8] J. L. Pan and C.G. Fonstad, *IEEE J. Quantum Electronics*, **35**, (1999), 1673.

[9] S. R. Andrews and B. A. Miller, *J. Appl. Phys.*, **70**, (1991), 993.

[10] V. Ryzhii, M. Rhyzii and H. C Liu, *J. Appl. Phys.*, **92**, (2002), 207.

[11] Sa'ar, C.Maemelstein, H. Schneider, C. Schoenbein, and M. Walther, *IEEE Photon.Technol. Lett.*, **10**, (1998), 1470.

[12] Thibaudeau, P. Bois, and J. Y. Duboz, *J. Appl. Phys.*, **79**, (1996), 446.

[13] E. Rosencher, F. Luc, Ph. Bois, and S. Delaitre, *Appl. Phys. Lett.*, **61**, (1992), 468.

[14] M. Ryzhii and V. Ryzhii, *IEEE Trans. Electron Devices*, **47**, (2000), 1935.

[15] G.S. Fishman, *Monte Carlo: Concepts, Algorithms, and Applications*, (Springer-Verlag, New York, 1996).

[16] M. Artaki and I. C. Kizilyalli, *Appl. Phys. Lett.*, **58**, (1991), 2467.

[17] M. Ryzhii and V. Ryzhii, *Physica E*, **7**, (2000), 120.

[18] M. Ryzhii and V. Ryzhii, *Jpn. J. Appl. Phys.*, **38**, (1999), 5922.

[19] M. Ryzhii and V. Ryzhii, *Appl. Phys. Lett.*, **72**, (1998), 842.

[20] M. Ryzhii, I. Khmyrova, and V. Ryzhii, *Jpn. J. Appl. Phys.*, **37,** (1998), 78.

[21] M. Ryzhii, V. Ryzhii, and M. Willander, *J. Appl. Phys.*, **84**, (1998), 3403.

[22] M. Ryzhii, V. Ryzhii, and M. Willander, *Jpn. J. Appl. Phys.*, **38**, (1999), 6650.

[23] M. Ryzhii, V. Ryzhii, R. Suris and C. Hamaguchi, *Jpn. J. Appl. Phys.*, **38**, (1999), L1388.

[24] M. Ryzhii, V. Ryzhii, Suris R and C.Hamaguchi, *Semicond. Sci. Technol.*, **16,** (2001), 202.

[25] S. D. Gunapala, S. V. Bandara, J. K. Liu, E. M. Luong, N. Stetson, C. A. Shott, J. J. Bock, S. B. Rafol, J. M. Mumolo, and M. J. Mckelvey, *IEEE Trans. Electron Devices*, **47**, (2000), 326.

[26] S. Adachi, *J. Appl. Phys.*, **58**, (1985), R1.

[27] K. K. Choi, *J. Appl. Phys.*, **73**, 5230, (1993).

[28] E. R. Brown, S. J. Eglash, and K. A. McIntosh, *Optoelectronic Properties of Semiconductors and Superlattices*, ed. M. Razeghi, vol. 1 (Gordon and Breach Science Publishers, Amsterdam, 1996) p.353.

[29] O. O. Cellek and C. Besikci, *Semicond. Sci. Technol.*, **19**, (2004), 183.

[30] O. O. Cellek, S. Memis, U. Bostanci, S. Ozer, C. Besikci, *Physica E*, **24**, (2004), 318.

[31] M. A. Khalil, M. Goano, A. Champagne, and R. Maciejko, *IEEE Photon. Technol. Lett.*, **8**, (1996), 19.

[32] J. L. Thobel, A. Sleiman, P. Bourel, and F. Dessenne, *J. Appl. Phys.*, **80**, (1996), 928.

[33] J. L. Educato, J. P. Leburton, J. Wang, and D. W. Bailey, *Phys. Rev. B*, **44**, (1991), 8365.

[34] S. M. Goodnick, and P. Lugli, *Phys. Rev. B*, **37**, (1988), 2578.

[35] C. Besikci, A. T. Bakir, and B. Tanatar, *J. Appl. Phys.*, **88**, (2000), 1504.

[36] S. Datta, *Quantum Phenomena* (Addison-Wesley, Reading, MA, 1989).

[37] D. Schroeder, *IEEE T. Comput. Aid. D.*, **9**, (1990), 1136.

[38] R. W. Hockney, and J. W. Eastwood, *Computer Simulation Using Particles* (Adam Hilger, Bristol, 1988).

[39] M. Ershov, H. C. Liu, M. Buchanan, Z. R. Wasilewski, and V. Ryzhii, *Appl. Phys. Lett.,* **70**, (1997), 414.

[40] H. Schneider, C. Mermelstein, R. Rehm, C. Schonbein, A. Sa'ar, and M. Walther, *Phys. Rev. B,* **57**, (1998), R15096.

[41] B. F. Levine, A. Zussman, S. D. Gunapala, M. T. Asom, J. M. Kuo, and W. S. Hobson, *J. Appl. Phys.*, **72**, (1992), 4429.

[42] G. Sarusi, S. D. Gunapala, J. S. Park, and B. F. Levine, *J. Appl. Phys.*, **76**, (1994), 6001.

[43] R. Rehm, H. Schneider, M. Walther, and P. Koidl, *Appl. Phys. Lett.*, **80**, (2002), 862.

[44] R. Rehm, H. Schenider, K.Schwarz, M. Walther, P. Koidl and G. Weimann, *Proc. SPIE*, **4288**, (2001), 379.

[45] O. O. Cellek, Ph. D. Prestudy Report, Department of Electrical and Electronics Eng., Middle East Technical University, Ankara, Turkey, 2003.